Functional Evaluation of Heme Vinyl Groups in Myoglobin with Symmetric Protoheme Isomers†

Yasuhiro Mie,*,‡ Chiho Yamada,§ Georges P.-J. Hareau,§ Saburo Neya,|| Tadayuki Uno,‡ Noriaki Funasaki,⊥ Katsuhiko Nishiyama,§ and Isao Taniguchi§

Graduate School of Pharmaceutical Sciences, Kumamoto University, 5-1, Oe-honmachi, Kumamoto 862-0973, Japan, Department of Applied Chemistry and Biochemistry, Kumamoto University, 2-39-1, Kurokami, Kumamoto 860-8555, Japan, Department of Physical Chemistry, Graduate School of Pharmaceutical Sciences, Chiba University, Inage-Yayoi, Chiba 263-8522, Japan, and Department of Physical Chemistry, Kyoto Pharmaceutical University, Yamashina, Kyoto 607-8414, Japan

Received May 11, 2004; Revised Manuscript Received August 2, 2004

ABSTRACT: We replaced protoheme-IX in native myoglobin with the symmetric protohemes-III and -XIII, in order to investigate the role of heme vinyl−globin contacts on Mb function. The UV−visible spectra and the resonance Raman spectra in the high-frequency region (containing oxidation, spin, and coordination state marker lines) of the two reconstituted Mbs were very similar. However, the signal intensity of the Soret band in the CD spectra and the resonance Raman lines for vinyl bending modes in the low-frequency region notably differed, thereby reflecting altered heme peripheral contacts. The redox potentials, formal heterogeneous electron-transfer rates, and thermal denaturation temperatures of the two reconstituted Mbs were also indistinguishable. In addition, the oxygen binding properties of the ferrous deoxy Mbs were comparable. These results demonstrate that altered heme vinyl−globin interactions only slightly affect the physical properties of Mb. It is therefore likely that the orientation of protoheme-IX about the α,γ-axis in the heme pocket is not necessarily a crucial factor for oxygen binding to native Mb.

Protoheme-IX (Figure 1) is an essential cofactor for hemoproteins, such as hemoglobin and myoglobin (Mb).[1] An X-ray analysis of Mb revealed that protoheme adopts a unique orientation in the heme pocket. However, NMR has revealed that the asymmetric protoheme-IX in Mb could assume normal and inverted orientations by rotating about the α,γ-meso carbon axis by 180° (Figure 1) (*1*, *2*). One of the orientational isomers has a higher stability than the other, and it dominates over time, after the reconstitution of Mb (*1*, *2*). There are two opinions regarding the heme disorder in Mb. One opinion is that the Mb containing the inverted protoheme-IX has a 10-fold greater O_2 affinity than the normal Mb, thereby emphasizing the importance of local heme−globin contacts (*3*). Another viewpoint is that the heme orientation does not significantly affect O_2 affinity (*4*).

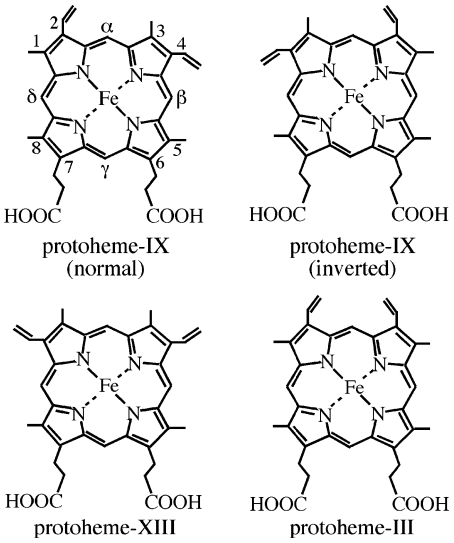

FIGURE 1: Structures of prosthetic groups.

The controversy appears to arise from the difficulty in accurately determining the fraction of inverted heme during equilibration. The protoheme accommodated in Mb in an opposite orientation alters the contacts between heme vinyls and surrounding globin, as illustrated in Figure 1.

Symmetric protohemes-III and -XIII, depicted in Figure 1, would provide useful insight for resolving the above-mentioned issue (*5*) because the orientation problem in the heme pocket is avoided. These hemes are excellent molecular tools for probing the microenvironment in the heme pocket; altered vinyl−globin interactions caused by protohemes-III

† This study was partially supported by a Grant-in-Aid from the Ministry of Education, Science, Sports and Culture, Japan, and research fellowships of the Japan Society for the Promotion of Science (JSPS) for Young Scientists to Y.M.

* To whom correspondence should be addressed. Current address: National Institute of Advanced Industrial Science and Technology, 2-17-2-1, Tsukisamu-higashi, Toyohira-ku, Sapporo 062-8517, Japan. Tel: +81-11-857-8913. Fax: +81-11-857-8915. E-mail: yasuhiro.mie@aist.go.jp.

‡ Graduate School of Pharmaceutical Sciences, Kumamoto University.

§ Department of Applied Chemistry and Biochemistry, Kumamoto University.

|| Chiba University.

⊥ Kyoto Pharmaceutical University.

[1] Abbreviations: CD, circular dichroism; CV, cyclic voltammogram; Mb, myoglobin; proto-III Mb, myoglobin reconstituted with protoheme-III; proto-XIII Mb, myoglobin reconstituted with protoheme-XIII.

10.1021/bi049051p CCC: $27.50
Published on Web 09/25/2004

and -XIII can mimic the situations produced on reorientation of protoheme-IX (Figure 1). A comparison of the two Mbs containing protohemes-III and -XIII, however, has not yet been reported because of the difficulties in preparing these symmetric protohemes. We have recently devised a method to synthesize protohemes-III and -XIII from common starting pyrroles (*6*). This improved method allows for the easy preparation of symmetric protohemes in large amounts. In this study, we report the first characterization of the two Mbs reconstituted with protoheme-III and -XIII. This provides an insight into the orientation problem of protoheme-IX in native Mb and the effects of heme vinyl−globin contacts on the function.

Among the various physical methods, functional electrodes are especially useful to direct electron transfer of metalloproteins (*7*−*9*), and electrochemical studies of semiartificial metalloproteins have investigated their electron-transfer reactions and biological functions (*10*−*12*). The electron-transfer reaction of Mb can be observed at an indium oxide electrode with a highly hydrophilic surface, and the biological functions and properties of Mbs reconstituted with heme and modified amino acid residues have been electrochemically studied (*12*−*16*).

MATERIALS AND METHODS

Preparation of Reconstituted Mbs. Horse heart Mb purchased from Sigma was purified by ion exchange chromatography (*17*, *18*). The concentration of aquomet Mb was estimated using $\epsilon_{409} = 188\ mM^{-1}\ cm^{-1}$ (*19*). Protoporphyrin-III and -XIII dimethyl esters were synthesized as previously described (*6*). Iron was inserted (*20*) and ester side chains were subsequently hydrolyzed (*21*) to yield protohemes-III and -XIII. ApoMb was prepared using acid methyl ethyl ketone (*22*, *23*). Protohemes-III and -XIII were dissolved in a minimum volume of 0.1 M NaOH, diluted with water, and mixed with apoMb at a molar ratio to apoMb of 1.5. The mixture was dialyzed against 10 mM bis-Tris buffer at pH 6.3. The reconstituted aquomet Mb was purified by cation exchange chromatography using CM-52 (Whatman) as described (*14*, *16*). The value of the ratio of the Soret band to the absorbance at 280 nm, above 5.4, was obtained for all the samples. Deoxy Mb was obtained by adding an excess of dithionite to aquomet Mb solution. Oxy Mb was prepared by passing deoxy Mb through an air saturated G-25 (Pharmacia Biotech) column equilibrated with Tris-HCl buffer (pH 7.0). The oxygen binding curve was obtained by adding buffer saturated with oxygen to the deoxy Mb prepared by photoirradiation (*24*).

Spectroscopy. The UV−visible and circular dichroism (CD) spectra were obtained using a Shimadzu UV-2100 spectrophotometer and a Jasco J-720 spectropolarimeter, respectively. The resonance Raman spectra were recorded using a double monochromator (Jasco R-800), following the excitation by a Krypton ion laser (406.7 nm line, Coherent I-302) with a laser power of 30 mW at the sample. Differential scanning calorimetry (DSC) was performed using a VP-DSC (MicroCal) calorimeter.

Electrochemistry. Cyclic voltammograms (CV) were obtained at 25 °C using a BAS CV-50W electrochemical analyzer at an In_2O_3 electrode (approximately $5 \times 5\ mm^2$, Kinoene Optics Corp., Japan) under an atmosphere of N_2. The electrode was cleaned by ultrasonication in 1% aqueous New-Vista (anionic surfactant, AIC Corp.), followed by ultrasonic washing in distilled water until the electrode surface became fully hydrophilic (*14*). A Pt plate and Ag/AgCl/saturated KCl were used as the counter and reference electrodes, respectively. The formal redox potential, $E^{\circ\prime}$, was evaluated as the midpoint of the anodic and cathodic peak potentials of the quasi-reversible redox wave. The formal heterogeneous electron-transfer rate constant, $k^{0\prime}$, and the dissociation rate constant of cyanide ions for Mb in the reduced form, k_f, were evaluated by CV simulation using BAS DigiSim software.

RESULTS

Spectral Properties. The coupling of apoMb with the symmetric protohemins successfully proceeded with >90% reconstitution yield owing to their high affinity. The electronic spectra of ferric proto-III and proto-XIII Mbs are closely similar to those of native Mb (*19*); this suggests that they are aquomet proteins with an iron-bound water molecule at neutrality. The water molecule of aquomet Mb dissociates into OH^- with an increase in pH. We examined the spectrophotometric pH titration of aquomet Mb to obtain structural information regarding the heme distal site. The acid−alkaline transition occurred at pH = 8.8 (±0.2) for proto-III Mb and pH = 8.9 (±0.2) for proto-XIII Mb (data not shown). These pH values indicate that the distal environments in the reconstituted Mbs are quite similar to those in the native Mb, since the acid−alkaline transition is closely affected by the distal histidine in Mb. This residue is essential for the stable accommodation of an exogenous oxygen molecule, implying that the reconstituted Mbs are capable of binding oxygen with an affinity similar to that of native Mb. The Mbs were stable at room temperature. The thermal stability was quantitatively monitored by DSC. Denaturation temperatures were 80.2 (±0.2) and 79.7 (±0.2) °C for proto-III Mb and proto-XIII Mb, respectively.

We recorded the resonance Raman spectra of the reconstituted Mbs in order to investigate the effect of heme replacements. The resonance Raman spectra of proto-III, proto-XIII, and native Mbs are shown in Figure 2. Resonance Raman spectroscopy is a powerful tool to reveal the oxidation, spin, and coordination states of heme iron (*25*−*27*). The ν_4 Raman line, an oxidation marker, appeared at approximately 1372 and 1356 cm^{-1} for ferric and ferrous hemes, respectively, as shown in Figure 2. Both proto-III and proto-XIII Mbs in the ferric form exhibited the ν_3 and ν_2 modes, which are the marker bands for coordination and spin states, at 1482 and 1564 cm^{-1}, respectively. In the deoxy forms, $\nu_3 = 1475\ cm^{-1}$ and $\nu_2 = 1565\ cm^{-1}$ were observed in proto-III Mb and the corresponding bands were observed at 1472 and 1563 cm^{-1} in proto-XIII Mb. These positions are similar to $\nu_3 = 1474\ cm^{-1}$ and $\nu_2 = 1564\ cm^{-1}$ of native Mb. The iron−histidine stretching mode ν(Fe−His) of deoxy heme was at 222 and 221 cm^{-1} for proto-III and proto-XIII Mbs, respectively, identical to that for native Mb (222 cm^{-1}) (*28*). Thus, reconstituted hemes are revealed to have essentially the same coordination structure as that in native Mb. The stretching and bending modes for vinyl groups are also included in the resonance Raman spectra, and the frequencies of those modes for ferric hemes have been assigned by Hu et al. (*29*). According to their paper, the line

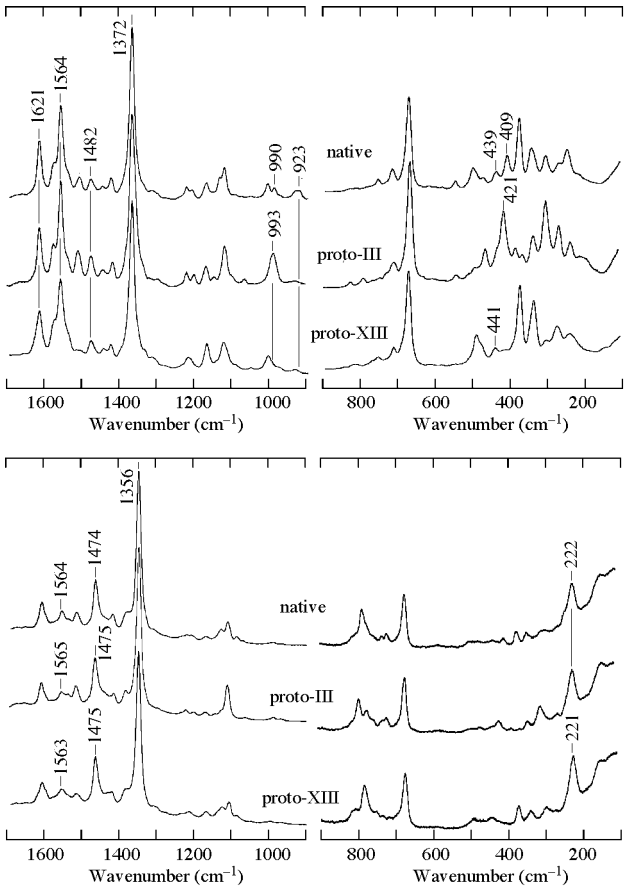

FIGURE 2: Resonance Raman spectra of 100 μM proto-III, proto-XIII, and native Mbs in both oxidized (upper) and reduced (lower) forms in a 100 mM phosphate buffer (pH 6.5) at room temperature. Laser excitation line, 406.7 nm (krypton ion laser); laser power, 30 mW at sample.

that appeared at 1621 cm^{-1} in the spectrum of native Mb was assigned to the vinyl ν(C=C) stretching mode. Both proto-III and proto-XIII Mbs also showed lines at 1621 cm^{-1} (Figure 2). In the low-frequency region, the out-of-plane γ-(C_aH=) wagging, the symmetric γ(=C_bH_2)$_s$ wagging, and the in-plane δ($C_\beta C_aC_b$) bending modes for vinyl chains appeared at 990, 923, and 439 cm^{-1}, respectively (and another δ($C_\beta C_aC_b$) signal also appeared at 409 cm^{-1}), for native Mb. These modes shifted or disappeared in the spectra of proto-III and proto-XIII Mbs and were clearly differentiated among the three Mbs.

We further recorded the CD spectra of the ferric and ferrous forms of native and reconstituted Mbs in order to monitor the difference in the heme peripheral contacts (*4*, *30*). Figure 3 shows that although their positions are almost the same, the Soret CD peak intensities increased in the following order: proto-III Mb (5.8×10^4 and 8.6×10^4 deg cm^2 dmol^{-1} for ferric and ferrous forms, respectively) < proto-XIII Mb (8.5×10^4 and 10×10^4 deg cm^2 dmol^{-1} for ferric and ferrous forms, respectively) < native Mb (11×10^4 and 13×10^4 deg cm^2 dmol^{-1} for ferric and ferrous forms, respectively). The intensity change is not surprising, since the Soret CD band mainly reflects the interaction between the heme and the aromatic side chains in the heme pocket (*30*). Santucci et al. have previously measured the CD spectrum of proto-XIII Mb and reported that the Soret signal intensities of proto-XIII Mb derivatives are significantly less than those of native Mb derivatives (*31*). Our

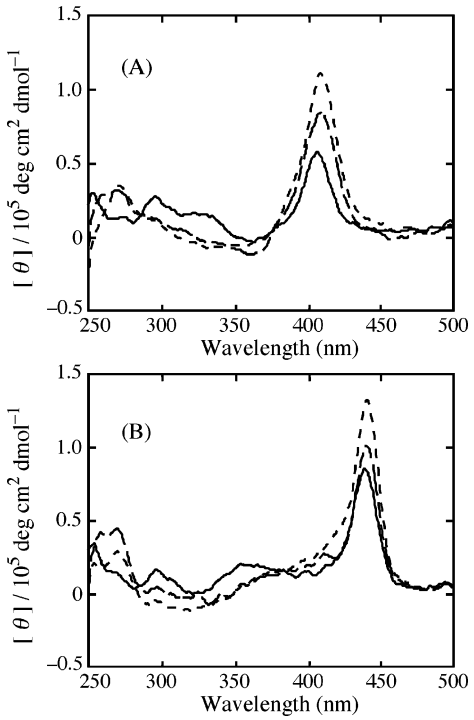

FIGURE 3: CD spectra of 25 μM proto-III (—), proto-XIII (– – –), and native (- - -) Mbs in both oxidized (A) and reduced (B) forms, in 100 mM bis-Tris buffer (pH 6.5) using a 0.2 cm cell.

CD results were essentially the same as theirs. Thus it is now clear that the reconstituted hemes have a similar structure in the heme pocket, although the peripheral interactions with the surrounding protein matrix differ markedly.

Kinetic Study for Heme Orientation. Since CD and resonance Raman spectroscopy are able to detect the difference in heme−globin contacts, we carried out the spectral measurements (including UV−visible spectroscopy) following the insertion of the protoheme into apoMb as a function of time. These measurements may reveal the existence of a metastable orientational isomer in Mb. No significant spectral change was observed in the UV−visible spectra of all the Mbs (proto-III, -IX, and -XIII) after 5 min mixing of each protoheme with apoMb. This indicated that under the present conditions the heme insertion was almost complete within this time. In the CD spectra, proto-III and -XIII Mbs demonstrated no change in the spectrum with time; however, the signal intensity in the Soret region of the proto-IX Mb increased with time, indicating a heme orientational change after its incorporation into Mb. After 3 h of mixing with apoMb, the spectrum of protoheme-IX was close to that of native Mb under the present conditions. In order to obtain a clearer understanding of this heme orientational change, kinetic measurements of the resonance Raman spectra were examined. Proto-III and -XIII Mbs exhibited no spectral change with time; however, proto-IX Mb displayed a significant change, especially in the vinyl in-plane bending frequencies around 409 and 439 cm^{-1}, as shown in Figure 4. These frequencies gradually converted to those of native Mb, thus revealing the existence of a metastable orientational isomer and a change in heme vinyl−globin contacts with time.

Electrochemical Properties. Direct electrochemistry is a powerful tool to evaluate redox potential, electron-transfer

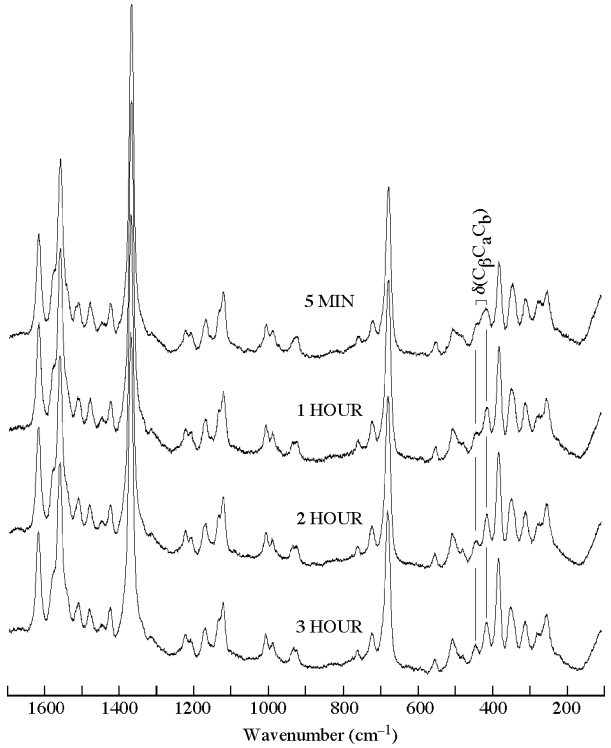

FIGURE 4: Time dependence of resonance Raman spectrum of protoheme-IX reconstituted myoglobin at pH 5.6 (0.1 M bis-Tris buffer solution). A 2-fold excess of apoMb was mixed with ferric heme. The final heme concentration was 100 μM. Laser excitation line, 406.7 nm; laser power, 30 mW at sample.

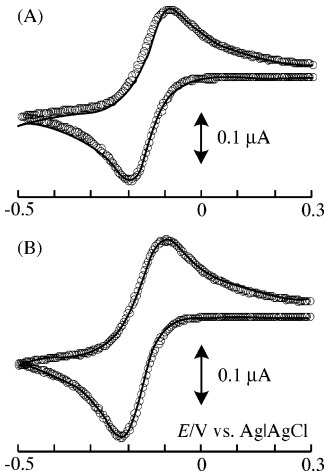

FIGURE 5: Background-subtracted cyclic voltammograms of (A) proto-XIII and (B) proto-III Mbs at an In_2O_3 electrode in 0.1 M bis-Tris buffer (pH 6.5) and a scan rate of 20 mV s^{-1} at 25 °C, together with simulated data (shown in circles) for indicated $k^{0\prime}$ values. $E^{\circ\prime}$ and D values used for simulation: (A) −0.145 V vs Ag/AgCl, 0.9 × 10^{-6} cm^2 s^{-1}, and (B) −0.160 V vs Ag/AgCl, 0.9 × 10^{-6} cm^2 s^{-1}, respectively, and 0.52 for α (transfer coefficient) in all situations.

kinetics, and chemical reaction(s) in proteins upon electron-transfer reaction (*9*, *12*, *16*). We measured the direct electrochemical activities of Mbs in the presence and absence of an exogenous ligand.

Figure 5 shows the redox waves in proto-III and proto-XIII Mbs at a highly hydrophilic In_2O_3 electrode surface. The waves were as well-defined as those of native Mb (*14*). The peak currents were linear with Mb concentrations over 25−100 μM and with the square root of the scan rate up to

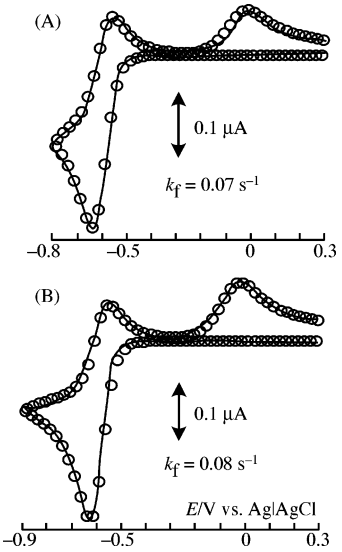

FIGURE 6: Background-subtracted cyclic voltammograms of cyano-Mbs for (A) proto-XIII and (B) proto-III at an In_2O_3 electrode and a scan rate of 20 mV s^{-1} at 25 °C, together with simulated data (shown in circles) for indicated k_f values, as shown in the text. $E^{\circ\prime}$ and D values used for simulation: (A) −0.600 V vs Ag/AgCl, 1.0 × 10^{-6} cm^2 s^{-1} and (B) −0.590 V vs Ag/AgCl, 1.0 × 10^{-6} cm^2 s^{-1}, respectively, and 0.50 for α (transfer coefficient) in all situations.

50 mV s^{-1}, indicating that the electrode reaction was diffusion-controlled. At 25 °C, the diffusion coefficients of proto-III and proto-XIII Mbs, estimated by both cyclic voltammetry and potential-step chronocoulometry, were approximately 1.0 (± 0.2) × 10^{-6} cm^2 s^{-1}. These values closely agree with 1.1 × 10^{-6} cm^2 s^{-1} for sperm whale Mb (*32*). The $E^{\circ\prime}$ values, estimated from the midpoint of anodic and cathodic peak potentials of quasi-reversible redox waves, were −145 and −160 mV for proto-III Mb and proto-XIII Mb, respectively. We estimated the formal heterogeneous electron-transfer rate constants, $k^{0\prime}$, using digital simulations of the observed voltammograms. The $k^{0\prime}$ values were about 5.7 (±0.5) × 10^{-4} and 7.0 (±0.5) × 10^{-4} cm s^{-1} for proto-III Mb and proto-XIII Mb, respectively.

Figure 6 shows the ligand dissociation properties of the reconstituted Mbs as determined by cyclic voltammetry. The coordinated water molecule of aquomet Mb is easily replaced with cyanide to give cyanomet Mb. The redox potentials of Mbs largely shifted to the negative direction on cyanide addition because CN^- donates a negative charge to the heme iron (Figures 5 and 6). After the reduction of cyanomet Mb, cyanide ions are released from the ferrous iron because CN^- has only a weak affinity (*13*, *16*, *33*):

$$\text{Mb(Fe(III))}-\text{CN}^- + \text{e} = \text{Mb(Fe(II))}-\text{CN}^- \quad (1)$$

$$\text{Mb(Fe(II))}-\text{CN}^- \rightarrow \text{Mb(Fe(II))} + \text{CN}^- \quad (2)$$

Figure 6 shows two reoxidation peaks in the voltammograms of cyano-Mbs at approximately −0.6 and 0 V for the oxidation of Mb(Fe(II))−CN^- and Mb(Fe(II)), respectively. The ratio of these oxidation currents depended on the potential sweep rate. At a slow scan rate, the peak around −0.6 V decreased and that around 0 V increased. We estimated the dissociation rate constant (k_f) of cyanide ions for eq 2, using a digital simulation of the observed voltammograms of cyano-Mbs. The calculated k_f values were 0.07

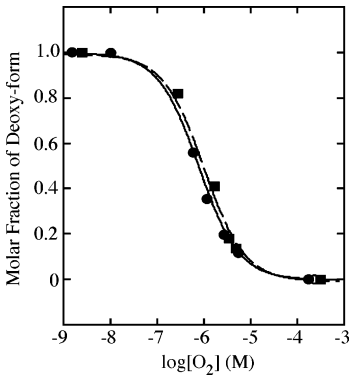

FIGURE 7: Oxygen titration profiles for proto-XIII (■, − − −) and proto-III (●, —) Mbs in 0.1 M phosphate buffer (pH 7.0) at 25 °C.

Table 1: Functional Parameters Obtained in This Study for Proto-III, Proto-XIII, and Native Mbs

Mb	$E^{\circ\prime}$ (mV)	$k^{0\prime}$ [a] $\times 10^4$ (cm s^{-1})	k_{auto} [b] $\times 10^5$ (s^{-1})	$k_f(CN^-)$ [c] (s^{-1})	K [d] $\times 10^{-7}$ (M^{-1})	pK_a [e]	T_m [f] (°C)
native	−140	6.5	8.0	0.10	7.9	8.7	81.5
proto-III	−160	5.7	8.1	0.08	12	8.8	80.2
proto-XIII	−145	7.0	6.5	0.07	10	8.9	79.7

[a] The formal heterogeneous electron-transfer rate constant at pH 6.5 and 25 °C. [b] The dissociation rate constant of CN^- from Mb(Fe(II)) at pH 7.5 and 25 °C. [c] The autoxidation rate constant of oxy Mb at pH 7.0 and 35 °C. [d] The equilibrium constant for oxygen binding at pH 7.0 and 25 °C. [e] The pK value for Mb(Fe−H_2O) = Mb(Fe−OH^-) at 25 °C. [f] Denaturation temperature measured at pH 7.0.

(±0.03) and 0.08 (±0.03) s^{-1} for proto-III and proto-XIII Mbs, respectively.

Functional Analysis. The Mbs reconstituted with symmetric protohemes reversibly bind oxygen; Figure 7 shows the oxygen binding profiles. Each titration fitted the theoretical curves with a Hill coefficient of 1.0. The oxygen affinities were 1.2 (±0.3) × 10^6 and 1.0 (±0.3) × 10^6 M^{-1} for proto-III Mb and proto-XIII Mb, respectively. We also examined the stability of oxy Mb against autoxidation. At pH 7.0 and 35 °C, the oxy Mb was gradually oxidized into aquomet protein, and the Soret peak shifted from 417 to 409 nm through a clear isosbestic point at 415 nm. The first-order plots monitored at 417 nm resulted in straight lines and rate constants for autoxidation, which were 8.1 (±0.5) × 10^{-5} and 6.5 (±0.5) × 10^{-5} s^{-1} for proto-III and proto-XIII Mbs, respectively. All the above spectroscopic, electrochemical, and functional results are complied in Table 1, together with those for native Mb.

DISCUSSION

Heme Environmental Structure. The visible absorption spectra and the resonance Raman spectra in the high-frequency region of the two Mbs containing the symmetric protoheme isomers are almost indistinguishable. In addition, they are thermally as stable as native Mb. However, the CD spectroscopy clearly differentiates between them. This is because the Soret CD band of Mb is a measure of the interaction between the heme and the aromatic side chains in the heme pocket (*30*). The position of the heme vinyl group is an essential contributor to the CD spectrum. The Soret CD signals of proto-III and -XIII Mbs are significantly less intense (Figure 3). Light et al. reported (*4*) that the CD signal of Mb, which was freshly reconstituted with asymmetric protoheme-IX, is less intense than that of native Mb because the protoheme-IX is equally distributed in the normal and inverted orientations. Our results also confirmed this fact (described in the Results section). Our observations for proto-III and -XIII Mbs with altered locations of the vinyl groups are consistent with the results, which demonstrated that inverted protoheme-IX exhibits a less intense Soret CD band. The resonance Raman spectra provided us with more detailed information regarding the heme vinyl−protein interactions. The vinyl stretching υ(C═C) frequencies of the three Mbs were exactly the same, and the intensities did not differ significantly among the Mbs. Marozocchi and Smulevich have reported (*34*) that the υ(C═C) stretching frequency depends on the torsion angle between the vinyl and pyrrole double bonds, which is induced by specific protein interactions. The same υ(C═C) stretching frequency (1621 cm^{-1}) of the three Mbs indicates that the torsion angle of the vinyl group in Mb is negligibly affected by the substitution. This in turn indicates that the globin matrix does not significantly constrain the vinyl chains. Further support is provided by the fact that the three Mbs exhibited similar redox potential values. This is because the orientation of vinyl groups, with respect to the plane of the heme, significantly affects the redox potential (*35*). On the other hand, the frequencies of the vinyl bending mode in the low-frequency region were clearly affected by the substitution, supporting the viewpoint of different heme vinyl−globin contacts among the Mbs.

The visible and resonance Raman spectra for the ferric Mbs reveal that a water molecule is coordinated to the ferric iron. Similar pK_a values for the acid−alkaline transition indicate that the hydrogen bond between the distal histidine and the iron-bound water is least perturbed after substitution with the protohemin isomers. Resonance Raman spectroscopy further demonstrates that the magnitude of the proximal His−Fe bonds in the deoxy Mbs containing protohemes-III and -XIII is also unperturbed. This is fully consistent with the observation that no significant difference in the iron redox potentials was observed. The conserved axial coordination structure of the two reconstituted Mbs is supported by the results of the electron-transfer kinetics. Since the electron-transfer rates of Mbs mainly depend on the reorganization energy around the active site (*12*, *15*), the similar $k^{0\prime}$ values for the two Mbs imply that the same structural changes were generated during the redox reaction. We conclude that the altered heme−globin contacts resulting from the positional shift of the vinyl groups in protohemes-III, -IX, and -XIII negligibly affect the heme axial coordination structure of Mb.

Role of the Vinyl Side Chains. The role of the vinyl groups of protoheme-IX in hemoprotein has been a subject of continued interest. The interaction of the heme vinyl group with a nearby amino acid residue in hemoglobin was proposed to play an important role in its cooperative ligand binding process (*36*). The orientation of the vinyl substituents with respect to the heme plane was found to modulate their electron-withdrawing ability in cytochrome b_5 (*35*) and cytochrome-*c* peroxidase (*37*), thereby resulting in the alteration of their redox potentials.

An analysis of oxygen binding of Mb with inverted protoheme-IX, in order to understand the effect of altered heme vinyl−globin contacts on the Mb function, is difficult. This is because the inverted protoheme rapidly turns into

the normal orientation during oxygen binding. The problem associated with the protoheme-IX inversion can be avoided by using the symmetric protohemes-III and -XIII. We deduced the influence of the altered heme vinyl−globin contacts by comparing the structural and biological properties of the Mbs reconstituted with symmetric protohemes. Table 1 summarizes our findings, and the most remarkable of these was that the properties of proto-III and -XIII Mbs are similar to one another. This suggests that the translocation of heme vinyl chains only moderately affects oxygen binding. This result is explained on the basis of the close resemblance of the axial coordination structures of the Mbs containing protoheme-III, -IX, or -XIII. Consequently, this indicates that the orientation of protoheme-IX, irrespective of whether it is normal or inverted in the heme pocket, does not significantly affect Mb function. The similarity among the three Mbs supports the original view proposed by Light et al. (*4*) that the functional differences between the Mbs with protoheme in normal and inverted orientations are insignificant. Neya et al. (*38*) reported that the total disruption of the heme peripheral contacts by rapid heme rotation about the proximal His−iron bond in Mb negligibly affects oxygen binding. This indicates that fine structural recognition of globin for heme is not always necessary for Mb function. The present results for proto-III and proto-XIII Mbs are in agreement with the ideas proposed by Light et al. (*4*) and Neya et al. (*38*).

In summary, we were able to evaluate the role of the vinyl groups of protoheme-IX in Mb by utilizing protohemes-III and -XIII, which are readily available at present. These are symmetric molecules and are promising tools that allow for the translocation of the vinyl groups, without heme disorder, in various hemoproteins.

REFERENCES

1. La Mar, G. N., Davis, N. L., Parish, D. W., and Smith, K. M. (1983) Heme orientational disorder in reconstituted and native sperm whale myoglobin, *J. Mol. Biol. 168*, 887−896.
2. La Mar, G. N., Toi, H., and Krisshnamoorthi, R. (1984) Proton NMR investigation of the rate and mechanism of heme rotation in sperm whale myoglobin: evidence for intramolecular reorientation about a heme twofold axis, *J. Am. Chem. Soc. 106*, 6395−6401.
3. Livingstone, D. J., Davis, L. N., La Mar, G. N., and Brown, W. D. (1984) Influence of heme orientation on oxygen affinity in native sperm whale myoglobin, *J. Am. Chem. Soc. 106*, 3025−3026.
4. Light, W. R., Rohlfs, R. J., Palmer, G., and Olson, J. S. (1987) Functional effects of heme orientational disorder in sperm whale myoglobin, *J. Biol. Chem. 262*, 46−52.
5. Neya, S., Nakamura, M., Imai, K., Hori, H., and Funasaki, N. (1996) Functional comparison of the myoglobins reconstituted with symmetric deuterohemes, *Biochim. Biophys. Acta 1296*, 245−249.
6. Hareau, G. P.-J., Neya, S., Funasaki, N., and Taniguchi, I. (2002) New route to protoporphyrins III and XIII from common starting pyrroles, *Tetrahedron Lett. 43*, 3109−3111.
7. Taniguchi, I. (1997) Probing metalloproteins and bioelectrochemical systems, *Interface 4*, 34−37.
8. Hawkridge, F. M., and Taniguchi, I. (1995) The direct electron transfer reactions of cytochrome c at electrode surfaces, *Comments Inorg. Chem. 17*, 163−187.
9. Armstrong, F. A. (1990) Probing metalloproteins by voltammetry, in *Structure and Bonding* (Clarke, M. J., Goodenough, J. B., Ibers, J. A., Jorgensen, C. K., Mingos, D. M. P., Neilands, J. B., Palmer, G. A., Reinen, D., Sadler, P. J., Weiss, R., and Williams, R. J. P., Eds.) Vol. 72, pp 137−221, Springer-Verlag, Berlin.
10. Battistuzzi, G., Borsari, M., Loschi, L., Ranieri, A., Sola, M., Mondovi, B., and Marchesini, A. (2001) Redox properties and acid-base equilibria of zucchini mavicyanin, *J. Inorg. Biochem. 83*, 223−227.
11. Barker, P. D., Gleria, K. Di., Hill, H. A., and Lowe, V. J. (1990) Electron transfer reactions of metalloproteins at peptide-modified gold electrodes, *Eur. J. Biochem. 190*, 171−175.
12. Dyke, B. R. V., Saltman, P., and Armstrong, F. A. (1996) Control of myoglobin electron-transfer rates by the distal (nonbound) histidine residue, *J. Am. Chem. Soc. 118*, 3490−3492.
13. Cohen, D. J., King, B. C., and Hawkridge, F. M. (1998) Spectroelectrochemical and electrochemical determination of ligand binding and electron transfer properties of myoglobin, cyanomyoglobin, and imidazolemyoglobin, *J. Electroanal. Chem. 447*, 53−62.
14. Mie, Y., Sonoda, K., Neya, S., Funasaki, N., and Taniguchi, I. (1998) Electrochemistry of myoglobins reconstituted with azahemes and mesohemes, *Bioelectrochem. Bioenerg. 46*, 175−184.
15. Taniguchi, I., Sonoda, K., and Mie, Y. (1999) Electroanalytical chemistry of myoglobin with modification of distal histidine by cyanated imidazole, *J. Electroanal. Chem. 468*, 9−18.
16. Mie, Y., Sonoda, K., Kishita, M., Krestyn, E., Neya, S., Funasaki, N., and Taniguchi, I. (2000) Effect of rapid heme rotation on electrochemistry of myoglobin, *Electrochim. Acta 45*, 2903−2909.
17. Hardman, K. D., Eylar, E. H., Ray, D. K., Banaszak, L. J., and Gurd, F. R. N. (1966) Isolation of sperm whale myoglobin by low temperature fractionation with ethanol and metallic ions, *J. Biol. Chem. 241*, 432−442.
18. Hapner, K. D., Bradshaw, R. A., Hartzell, C. R., and Gurd, F. R. N. (1968) Comparison of myoglobins from harbor seal, porpoise, and sperm whale: I. preparation and characterization, *J. Biol. Chem. 243*, 683−689.
19. Antonini, E., and Brunori, M. (1971) *Hemoglobin and myoglobin in Their Reactions with Ligands*, pp 19 and 44, North Holland, Amsterdam,.
20. Chang, C. K., Dinello, R. K., and Dolphin D. (1989) Iron porphyrins, *Inorg. Synth. 20*, 147−151.
21. Fuhrhope, J. H., and Smith, K. M. (1975) Hydrolysis of esters, *Porphyrins Metalloporphyrins* 836−837.
22. Teale, F. W. J. (1959) Cleavage of heam-protein link by acid methylethylketone, *Biochim. Biophys. Acta 35*, 543.
23. Asakura, T. (1978) Hemoglobin porphyrin modification, *Methods Enzymol. 52*, 447−455.
24. Ward, B., and Chang, C. K. (1982) A convenient photochemical method for reduction of ferric hemes, *Photochem. Photobiol. 35*, 757−759.
25. Morikis, D., Champion, P. M., Springer, B. A., Egeberg, K. D., and Sligar, S. G. (1990) Resonance Raman studies of iron spin and axial coordination in distal pocket mutants of ferric myoglobin, *J. Biol. Chem. 265*, 12143−12145.
26. Kitagawa, T., Kyogoku, Y., Iizuka, T., and Saito, M. I. (1976) Nature of iron-ligand bond in ferrous low spin hemoproteins studied by resonance Raman scattering, *J. Am. Chem. Soc. 98*, 5169−5173.
27. Uno, T., Sakamoto, R., Tomisugi, Y., Ishikawa, Y., and Wilkinson, A. J. (2003) Inversion of axial coordination in myoglobin to create a proximal ligand binding pocket, *Biochemistry 42*, 10191−10199.
28. Peterson, E. S., Friedman, J. M., Chien, E. Y. T., and Sligar, S. G. (1998) Functional implications of the proximal hydrogen-bonding network in myoglobin: A resonance Raman and kinetic study of Leu89, Ser92, His97, and F-helix swap mutants, *Biochemistry 37*, 12301−12319.
29. Hu, S., Smith, K. M., and Spiro, T. G. (1996) Assignment of protoheme resonance Raman spectrum by heme labeling in myoglobin, *J. Am. Chem. Soc. 118*, 12638−12646.
30. Hsu, M.-C., and Woody, R. W. (1971) The origin of the heme Cotton effects in myoglobin and hemoglobin, *J. Am. Chem. Soc. 93*, 3515−3525.
31. Santucci, R., Ascoli, F., La Mar, G. N., Parish, D. W., and Smith, K. M. (1990) Horse heart myoglobin reconstituted with a symmetrical heme: a circular dichroism study, *Biophys. Chem. 37*, 251−255.
32. Crumpton, M. J., and Polson, A. (1965) A comparison of the conformation of sperm whale metmyoglobin with that of apomyoglobin, *J. Mol. Biol. 11*, 722−729.
33. Bellelli, A., Antonini, G., Brunori, M., Springer, B. A., and Sligar, S. G. (1990) Transient spectroscopy of the reaction of cyanide with ferrous myoglobin: effect of distal side residues, *J. Biol. Chem. 265*, 18898−18901.

34. Marzocchi, M., and Smulevich, G. (2003) Relationship between heme vinyl conformation and the protein matrix in peroxidases, *J. Raman Spectrosc. 34*, 725−736.
35. Reid, L. S., Lim, A. R., and Mauk, G. (1986) Role of heme vinyl groups in cytochrome b_5 electron transfer, *J. Am. Chem. Soc*. *108*, 8197−8201.
36. Perutz, M. F. (1976) Structure and mechanism of haemoglobin, *Br. Med. Bull*. *32*, 195−208.
37. Satterlee, J. D., and Erman, J. E. (1983) Temperature and pH dependence of the proton magnetic hyperfine resonance of cytochrome c peroxidase-cyanide, *J. Biol. Chem. 258*, 1050−1056.
38. Neya, S., Funasaki, N., Shiro, Y., Iizuka, T., and Imai, K. (1994) Consequence of rapid heme rotation to the oxygen binding of myoglobin, *Biochim. Biophys. Acta 1208*, 31−37.

BI049051P